

Comparison of the brilliance limit between MAX IV 3 GeV ring and NSLS II low beta straights using the same undulator technique

Erik Wallén*

Thu 10 Nov 2011 22:18:57

Contents

Contents	1
1 Introduction	2
2 Undulator technique used for the comparison	2
3 Ring parameters used for the comparison of the brilliance limit	4
4 Results of the comparison of the brilliance limit	4
5 Comparison of specific undulators at different synchrotron radiation storage rings	8
References	19
List of Tables	19
List of Figures	19

*Email: erik.wallén@maxlab.lu.se, Telephone +46 46 222 33 56, Address: E. Wallén, MAX-lab, Box 118, SE-22100 Lund, Sweden

1 Introduction

The brilliance of an undulator at a synchrotron radiation storage ring depends, in addition to the accelerator parameters, strongly on the undulator technique used. The accelerator parameters includes the vertical stay clear aperture and the available length for the undulators at the straight sections.

A smaller vertical stay clear aperture makes it possible to use a shorter period length and more periods along the length of the undulators. In vacuum undulators have for example a superior performance compared to out of vacuum standard undulators regarding the capacity to produce radiation with high brilliance at high photon energies.

The selection of undulators used at different synchrotron radiation is disperse and the selection of undulators used may not always be guided only by the search for the highest possible brilliance at as a short wavelength as possible. It would hence be difficult to base a comparison of the brilliance limit of different synchrotron radiation storage rings on the undulators in use. A better way to compare the brilliance limit between different synchrotron radiation storage rings is to use the same undulator technique for all rings in the comparison and let the boundary conditions for the undulators, i.e. the vertical stay clear aperture and available straight section length, determine the period length and number of periods of the undulator.

During the calculation of the brilliance limit, the undulator length is fixed while the undulator period length is varied to optimise the brilliance for each photon energy in the plot. In this way the brilliance limit for a specific undulator technique and storage ring can be found. The only way to increase the brilliance is to use a stronger magnetic material in the undulator or decrease the gap.

2 Undulator technique used for the comparison

To compare the brilliance limit for different storage rings I have used the same undulator technique as has been used in the PETRA III Technical Design Report[1], which is an approximative formula for the peak field in a hybrid type undulator with vanadium-permedur pole pieces derived by P. Elleaume, J. Chavanne, and Faatz [2]. The formula for the peak field B_0 in Tesla at the gap g and period length λ_0 is

$$B_0 = a \times \exp \left[b \frac{g}{\lambda_0} + c \left(\frac{g}{\lambda_0} \right)^2 \right] \quad (1)$$

where $a = 3.69$, $b = -5.07$, and $c = 1.52$. The K -value, or deflection parameter, is in analogy with the PETRA III Technical Design Report[1] written as

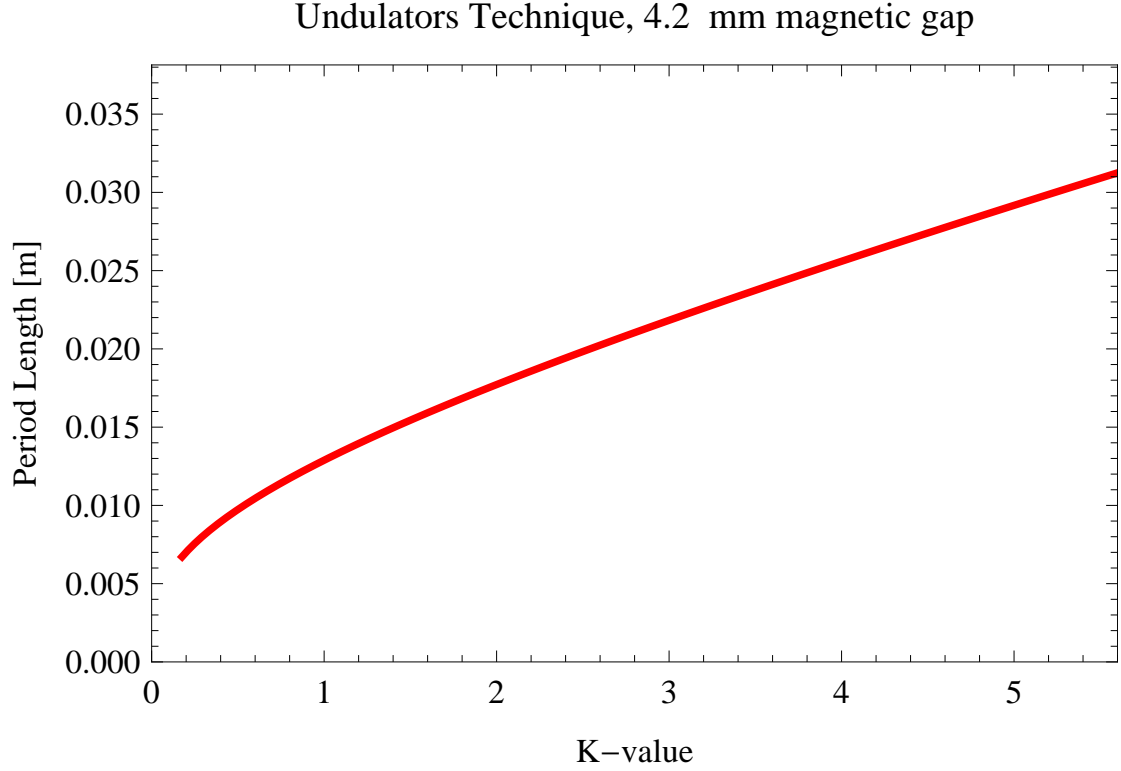


Figure 1: Limit at different gaps of the undulator technique used for the comparison of the brilliance limit

$$K = 0.934 \times \lambda_0[cm] \times B_0[T] \quad (2)$$

The use of the peak field and not the effective field for the calculation of the K -value of the undulator does probably give an overestimate of the K -value of 5-10 % since in hybrid devices the peak field in general is stronger than the efficient field.

The performance limit of the undulator technique is given by the minimum period length for specific K -value at the gap defined by the vertical stay clear aperture. In this set of calculations I have assumed that in-vacuum undulators with a magnetic gap 0.2 mm larger than than vertical stay clear aperture and a K -value in the range 0.2 to 7 are used. Figure 1 shows examples of the minimum period length depending on the K -value at different magnetic gaps.

3 Ring parameters used for the comparison of the brilliance limit

The parameters of the different synchrotron radiation storage rings in the comparison, MAX IV [3], NSLS II [4], PETRA III [1], ALS [5], DIAMOND [6], ESRF [7], SOLEIL [8], and MAX II [9], are shown in Table 1, where E is the energy of the stored beam, I is the beam current, σ_γ is the energy spread in the beam, ε_H and ε_V are the horizontal and vertical emittance of the beam, β_H and β_V are the values of the horizontal and vertical beta-functions in the middle of the straight section, L_{MAX} is the maximum available magnetic length of the insertion device, a_v is the vertical beam stay clear aperture. It is assumed that the undulators are situated in the middle of straight sections with negligible dispersion.

Table 1: Parameters used for the comparison of the brilliance limit at different light sources [3, 4, 1, 5, 6, 7, 8, 9]

Facility	E GeV	I A	σ_γ %rms	ε_H pmrad	ε_V pmrad	β_H m	β_V m	L_{MAX} m	a_v mm
MAX IV	3	0.5	0.1	263	8.	9.539	1.982	3.8	4
NSLS II	3	0.5	0.1	550	8.	1.5	0.8	3.8	4
PETRA III	6	0.1	0.1	1000	10.	1.3	3	3.8	6
ALS	1.9	0.4	0.1	6000	60.	11.2	4.2	3.8	8
DIAMOND	3	0.3	0.11	2740	27.4	18	5	3	5
ESRF	6	0.2	0.11	4000	24.	0.5	2.73	4	5
SOLEIL	2.75	0.3	0.1	3740	40	17.8	1.75	4	5
MAX II	1.5	0.2	0.2	8840	880.	13	2.5	2.2	8

4 Results of the comparison of the brilliance limit

The brilliance limit of the synchrotron radiation storage rings in Table 1 is shown in Figure 2.

The angular spectral flux at the brilliance limit of the synchrotron radiation storage rings in Table 1 is shown in Figure 3.

The ratio of coherent flux, where the jumps in the curve corresponds to jumps between different harmonic, of the synchrotron radiation storage rings in Table 1 is shown in Figure 4.

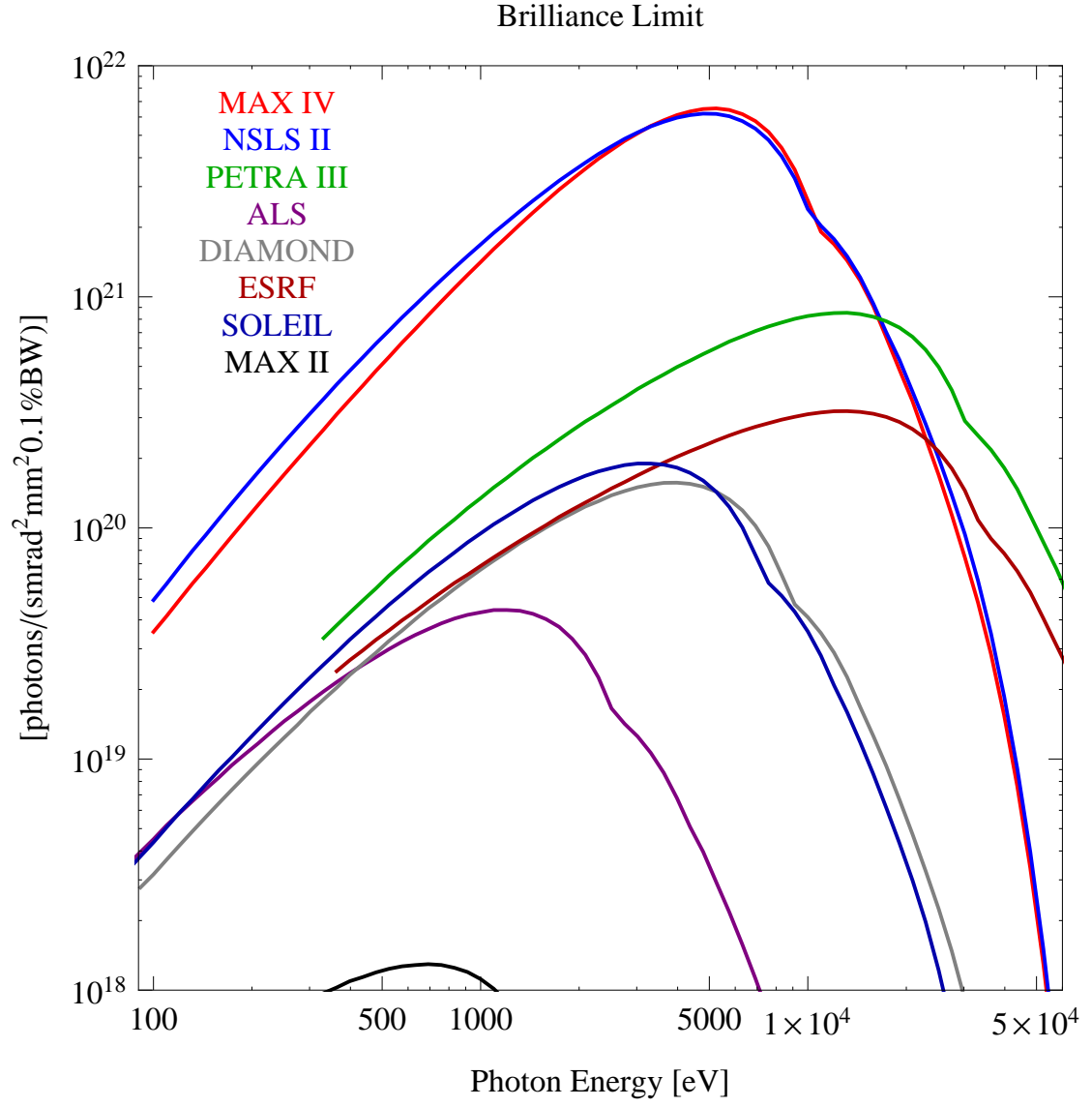


Figure 2: The brilliance limit of the synchrotron radiation storage rings in Table 1

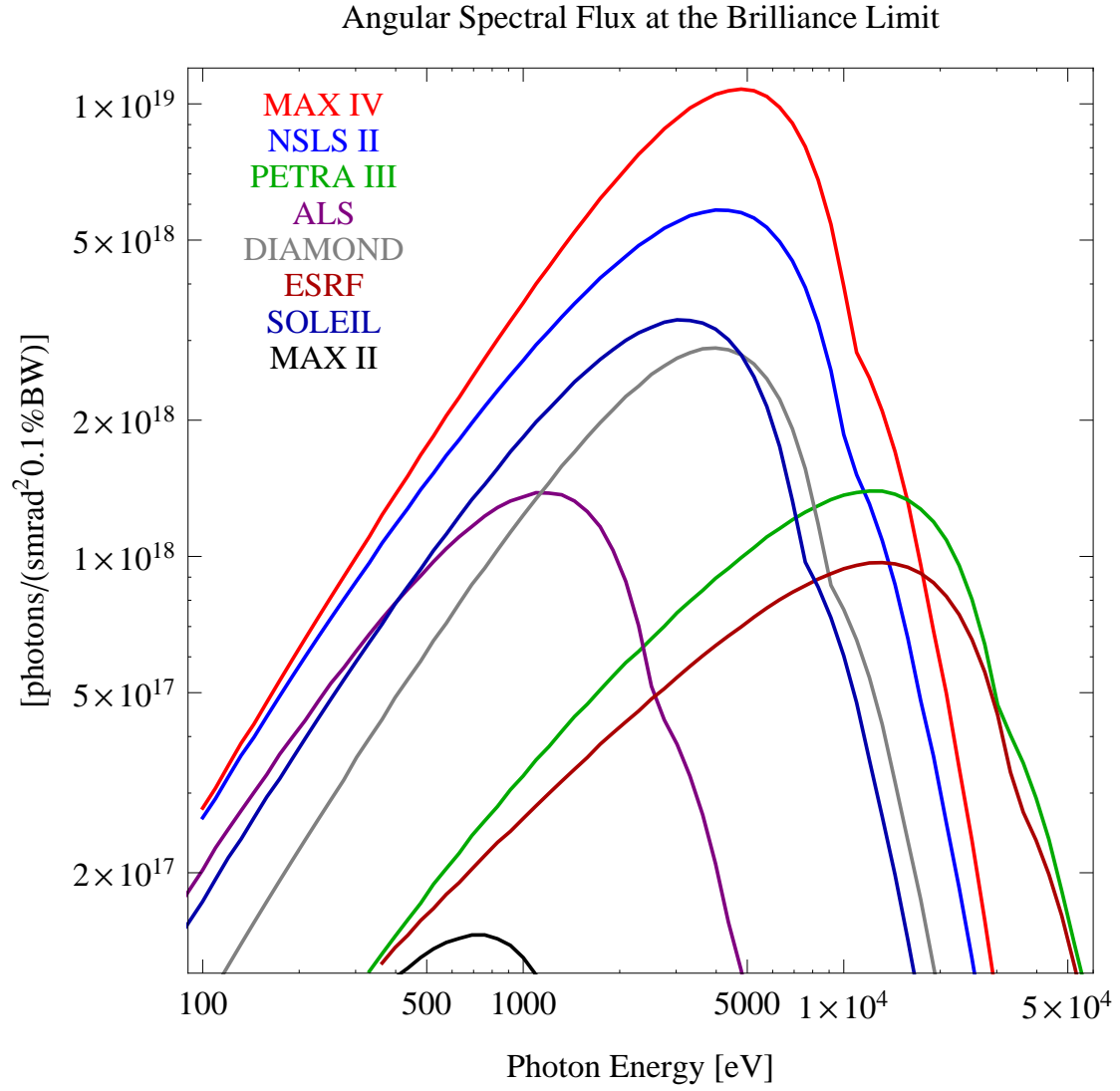


Figure 3: The angular spectral flux at the brilliance limit of the synchrotron radiation storage rings in Table 1

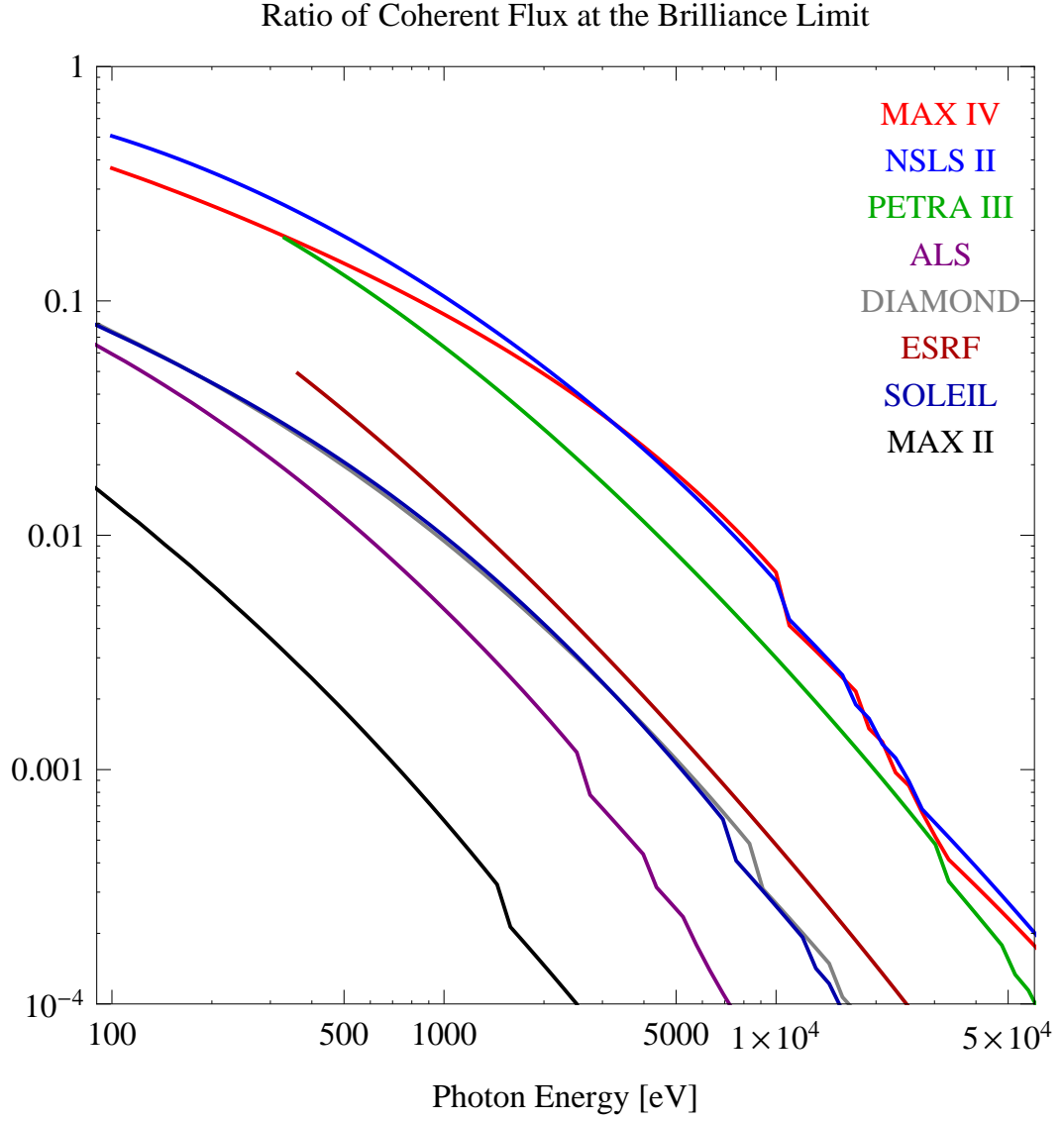


Figure 4: The ratio of coherent flux, where the jumps in the curve corresponds to jumps between different harmonic, of the synchrotron radiation storage rings in Table 1

5 Comparison of specific undulators at different synchrotron radiation storage rings

The performance of specific undulators at a selection of existing and future synchrotron radiation storage rings has been compared.

The selection of undulators at the synchrotron radiation storage rings, MAX IV [3], NSLS II [4], PETRA III [1], ALS [5], DIAMOND [6], ESRF [7], SOLEIL [8], and MAX II [9], is shown in Table 2, where E is the energy of the stored beam, I is the beam current, σ_γ is the energy spread in the beam, ε_H and ε_V are the horizontal and vertical emittance of the beam, β_H and β_V are the values of the horizontal and vertical beta-functions in the middle of the straight section, L_{ID} is the magnetic length of the insertion device, λ_0 is the period length, and K_{max} is the maximum K -value of the undulator. It is assumed that the undulators are situated in the middle of a straight section with negligible dispersion.

The choice of undulators is targeted towards the shortest existing period length at the different synchrotron radiation storage rings. The minimum K -value for the undulators during the calculations is 0.2 and the maximum K -value is given in Table 2.

Table 2: Parameters used for the comparison of specific undulators at different light sources [3, 4, 1, 5, 6, 7, 8, 9]

Facility	E GeV	I A	σ_γ %rms	ε_H pmrad	ε_V pmrad	β_H m	β_V m	ID/BL	L_{ID} m	λ_0 mm	K_{max}
MAX IV	3	0.5	0.1	263	8.	9.539	1.982	pmu18p5	3.8	18.5	1.92
NSLS II	3	0.5	0.1	550	8.	1.5	0.8	U19	3.	19.	2.03
PETRA III	6	0.1	0.1	1000	10.	1.3	3	U29	5.	29.	2.2
ALS	1.9	0.4	0.1	6000	60.	11.2	4.2	U8	4.4	80.	5.98
DIAMOND	3	0.3	0.11	2740	27.4	18	5	I03	1.98	21	1.69
ESRF	6	0.2	0.11	4000	24.	0.5	2.73	ID27	4	23	1.61
SOLEIL	2.75	0.3	0.1	3740	40	17.8	1.75	U20	1.8	20	1.92
MAX II	1.5	0.2	0.2	8840	880.	13	2.5	I1011	2.1	46.6	3.1

The brilliance at peak energy of the synchrotron radiation emitted at the rings and undulators in Table 2 is shown in Figure 5.

The angular spectral flux of the synchrotron radiation emitted at the rings and undulators in Table 2 is shown in Figure 6.

The flux of photons in the harmonics of the emitted synchrotron radiation at the rings and undulators in Table 2 using a 0.1%BW monochromator is shown in Figure 7.

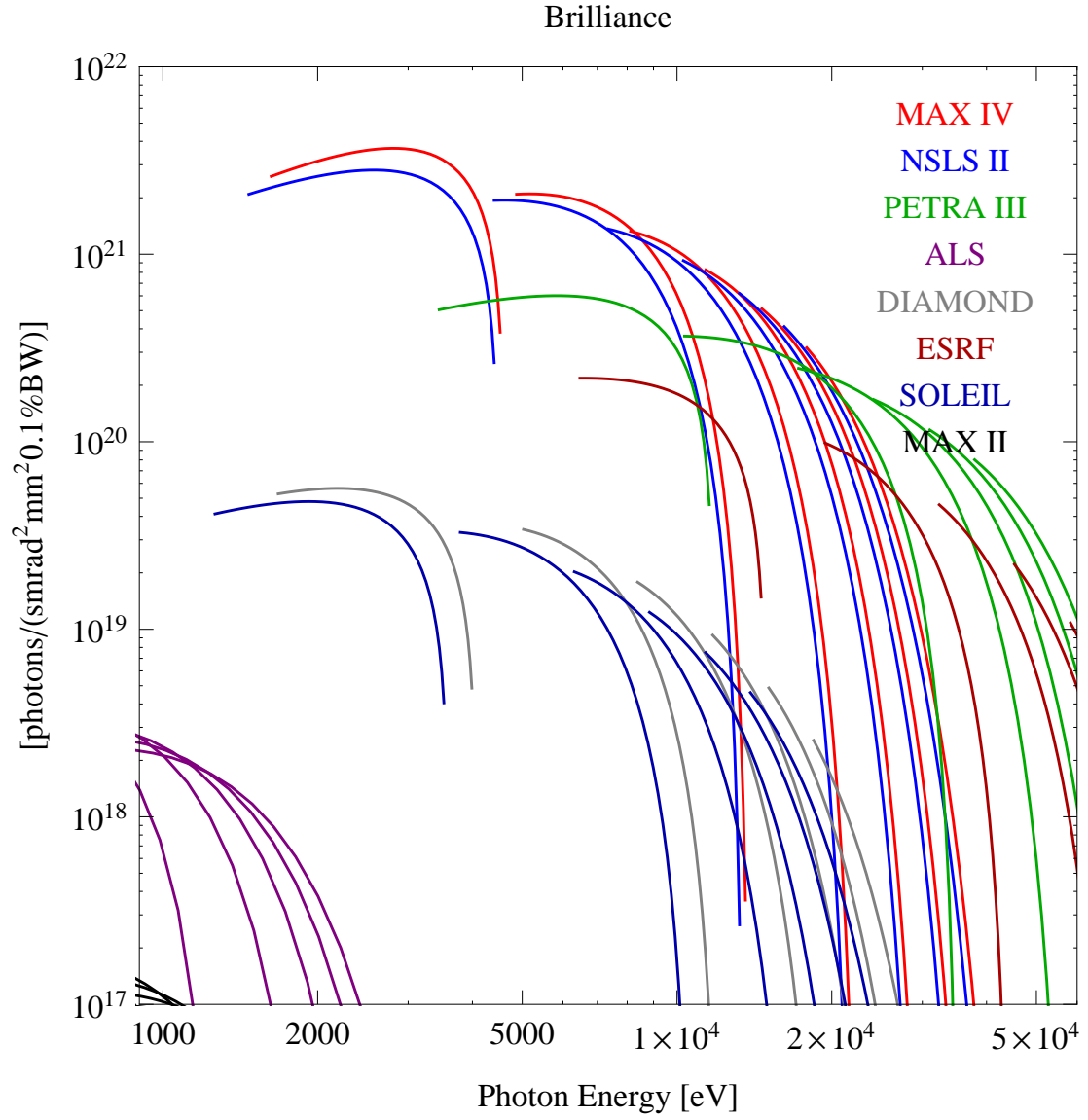


Figure 5: The brilliance at peak energy of the synchrotron radiation emitted at the rings and undulators in Table 2

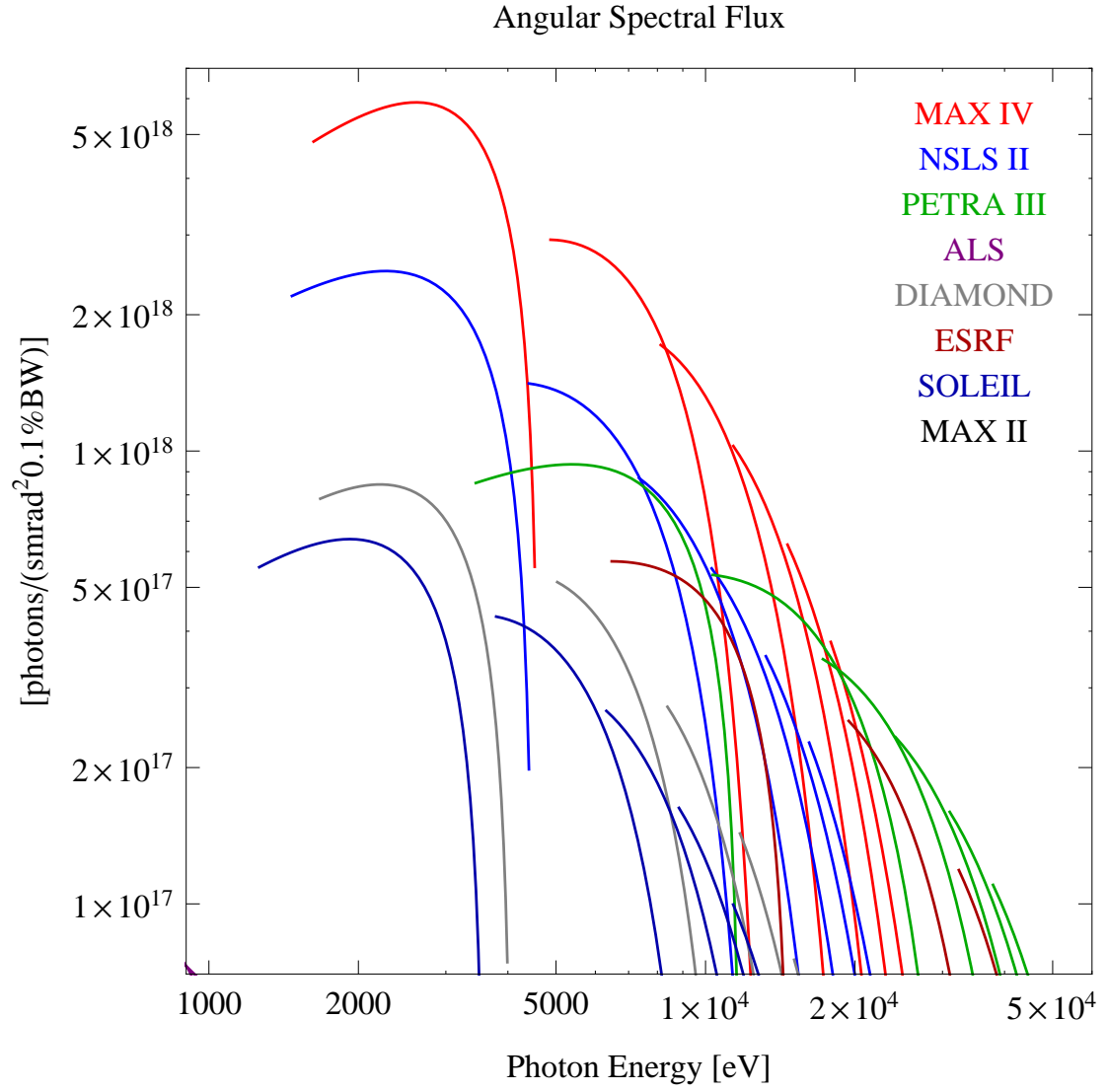


Figure 6: The angular spectral flux of the synchrotron radiation emitted at the rings and undulators in Table 2

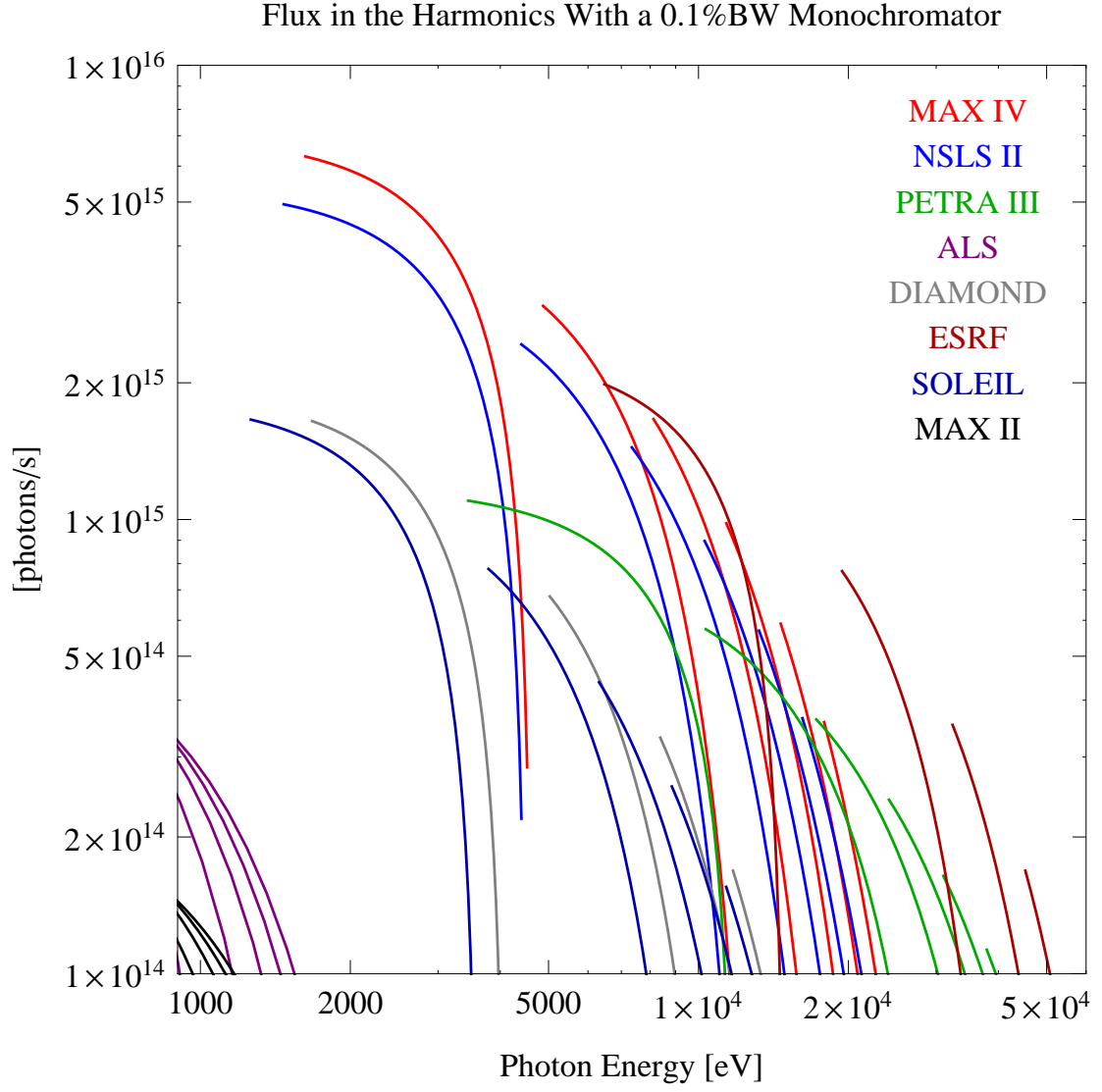


Figure 7: The flux of photons in the harmonics of the emitted synchrotron radiation at the rings and undulators in Table 2 using a 0.1%BW monochromator

The flux of photons in the harmonics of the emitted synchrotron radiation from the rings and undulators in Table 2 is shown in Figure 8.

The power in the harmonics of the emitted synchrotron radiation from the rings and undulators in Table 2 is shown in Figure 9.

The ratio of coherent flux in the harmonics of the emitted synchrotron radiation from the rings and undulators in Table 2 is shown in Figure 10.

The coherent flux in the harmonics of the rings and undulators in Table 2 using a 0.1%BW Monochromator is shown in Figure 11.

The coherent flux in the harmonics of the the rings and undulators in Table 2 is shown in Figure 12.

The power of coherent synchrotron radiation in the harmonics of the the rings and undulators in Table 2 is shown in Figure 13.

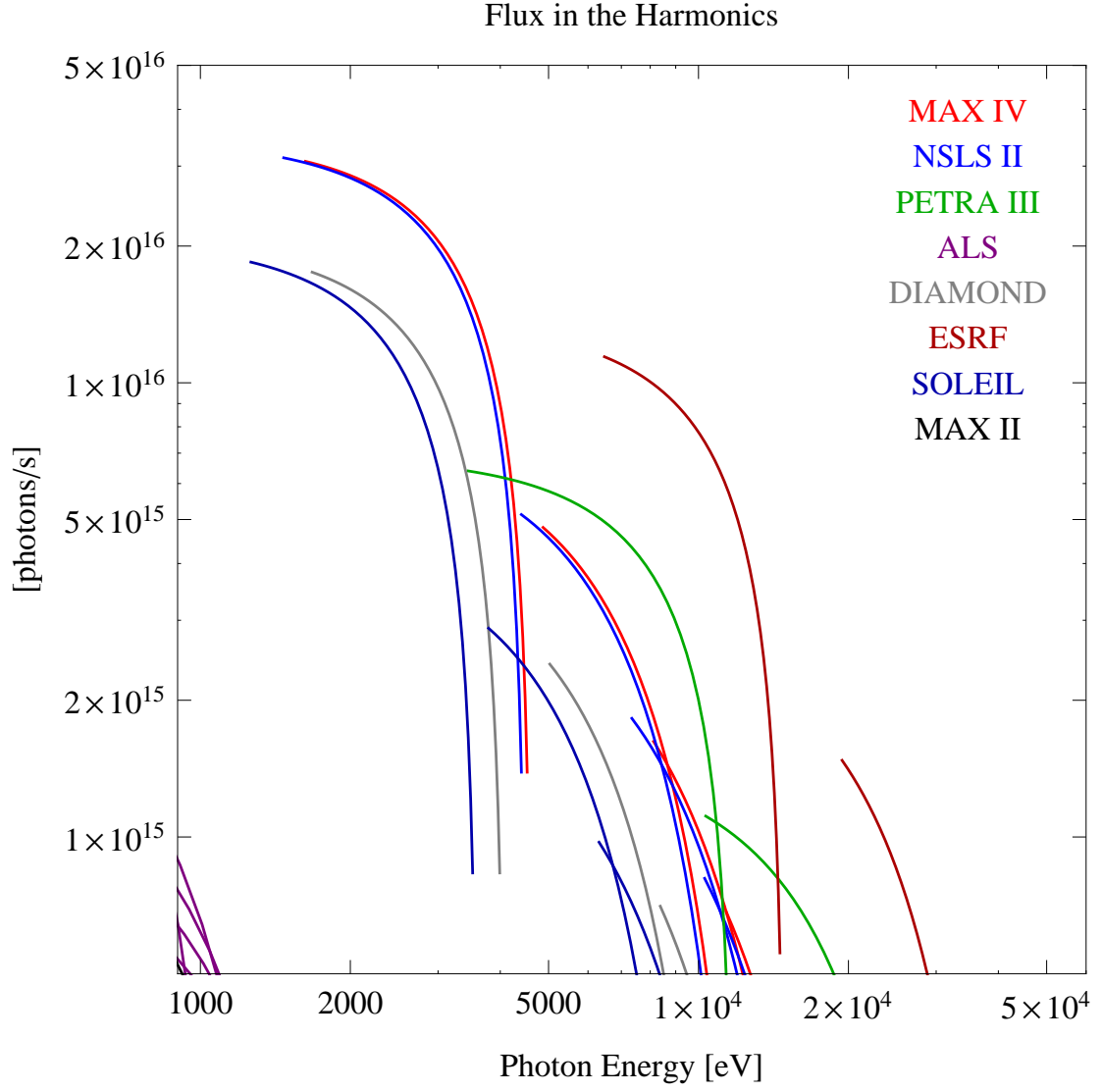


Figure 8: The flux of photons in the harmonics of the emitted synchrotron radiation from the rings and undulators in Table 2

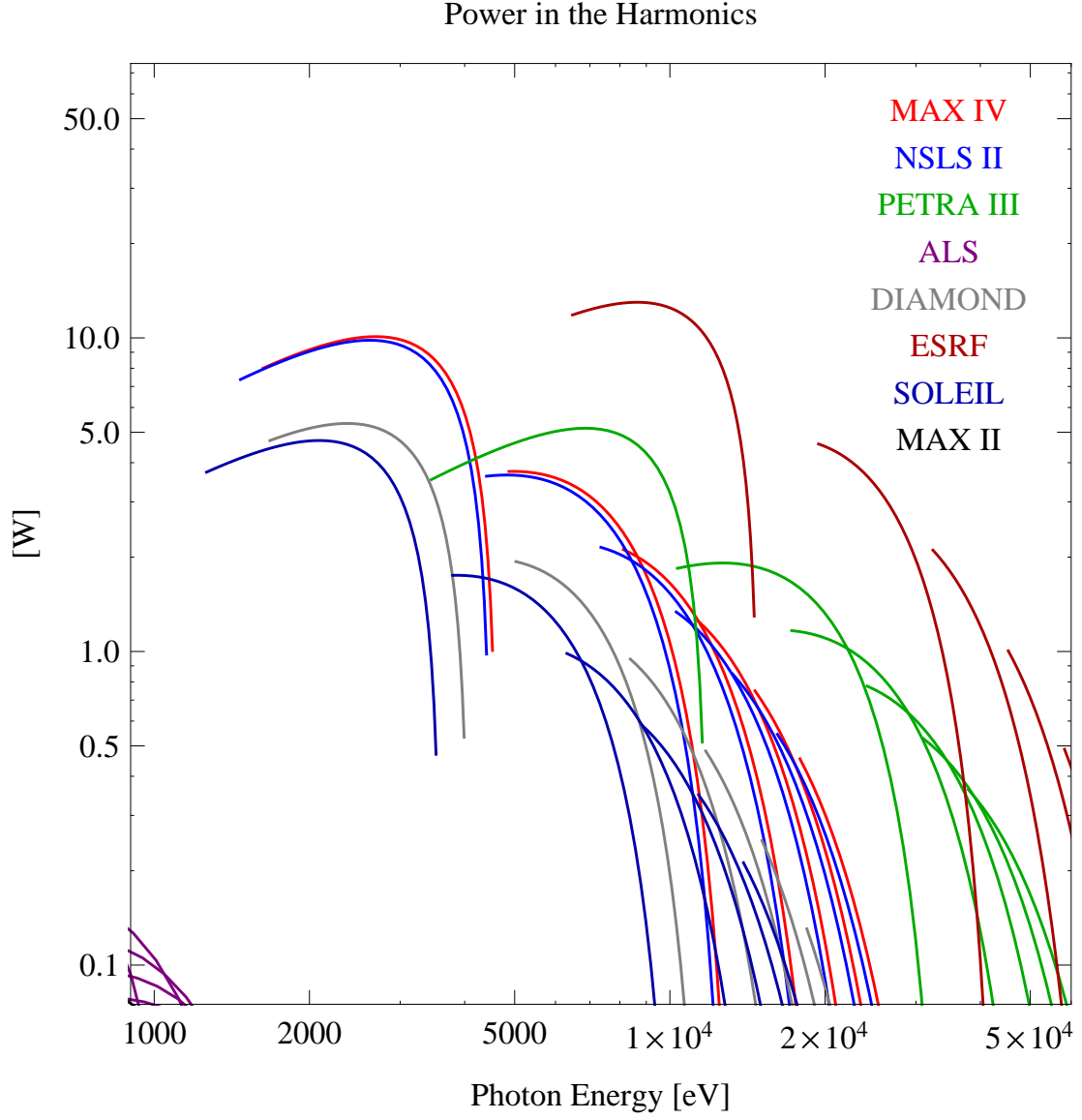


Figure 9: The power in the harmonics of the emitted synchrotron radiation from the rings and undulators in Table 2

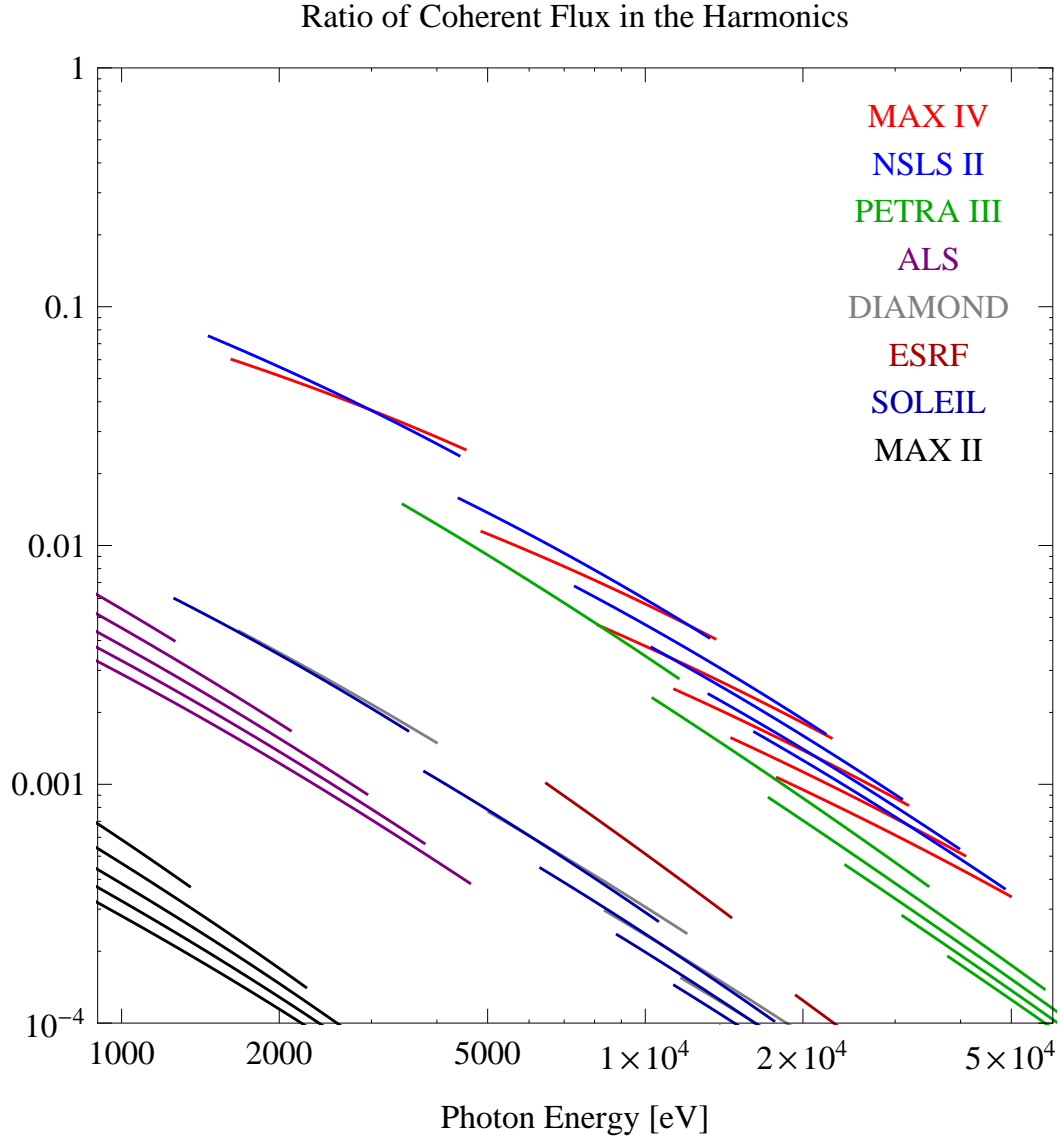


Figure 10: The ratio of coherent flux in the harmonics of the emitted synchrotron radiation from the rings and undulators in Table 2

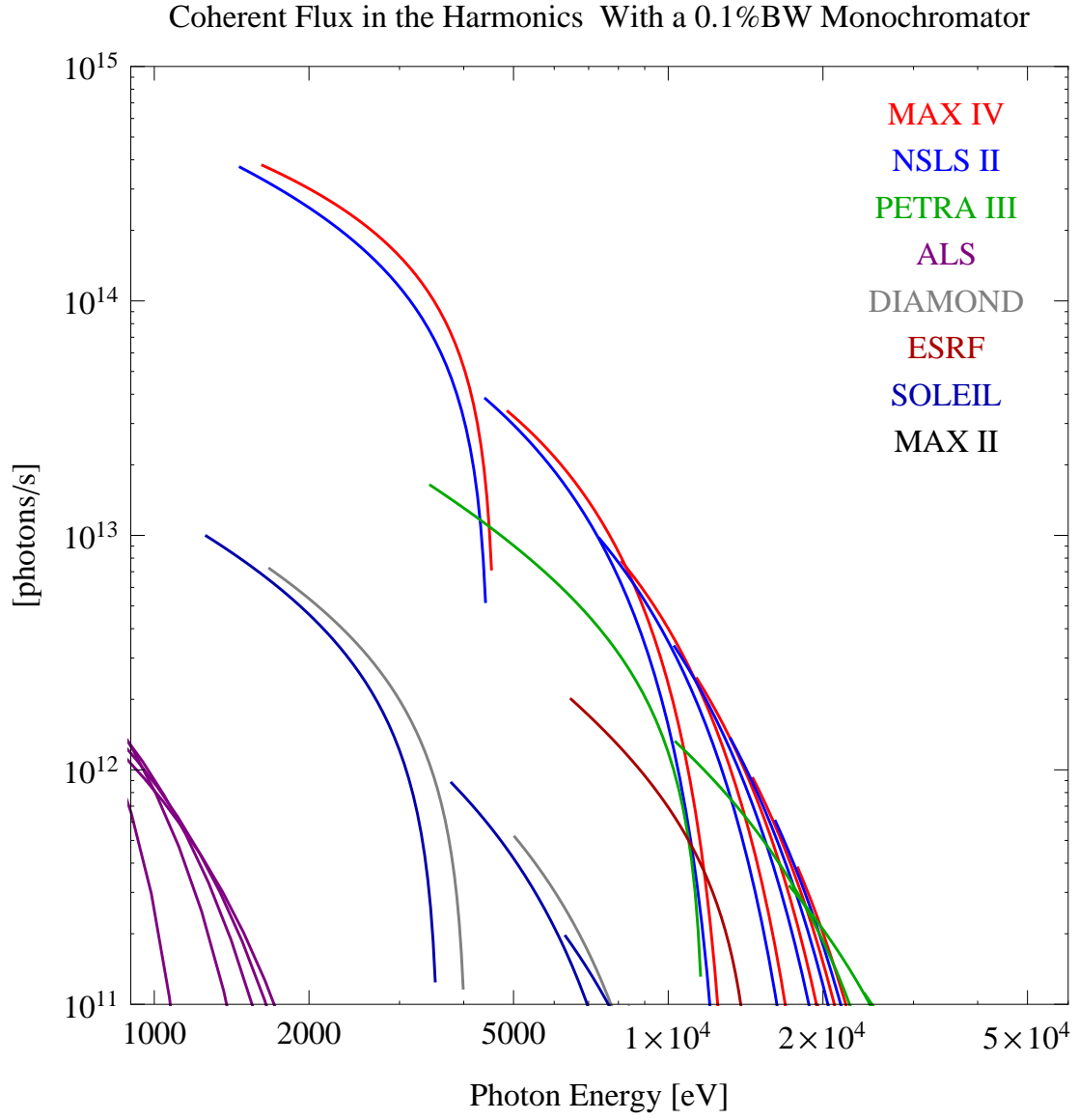


Figure 11: The coherent flux in the harmonics of the rings and undulators in Table 2 using a 0.1%BW Monochromator

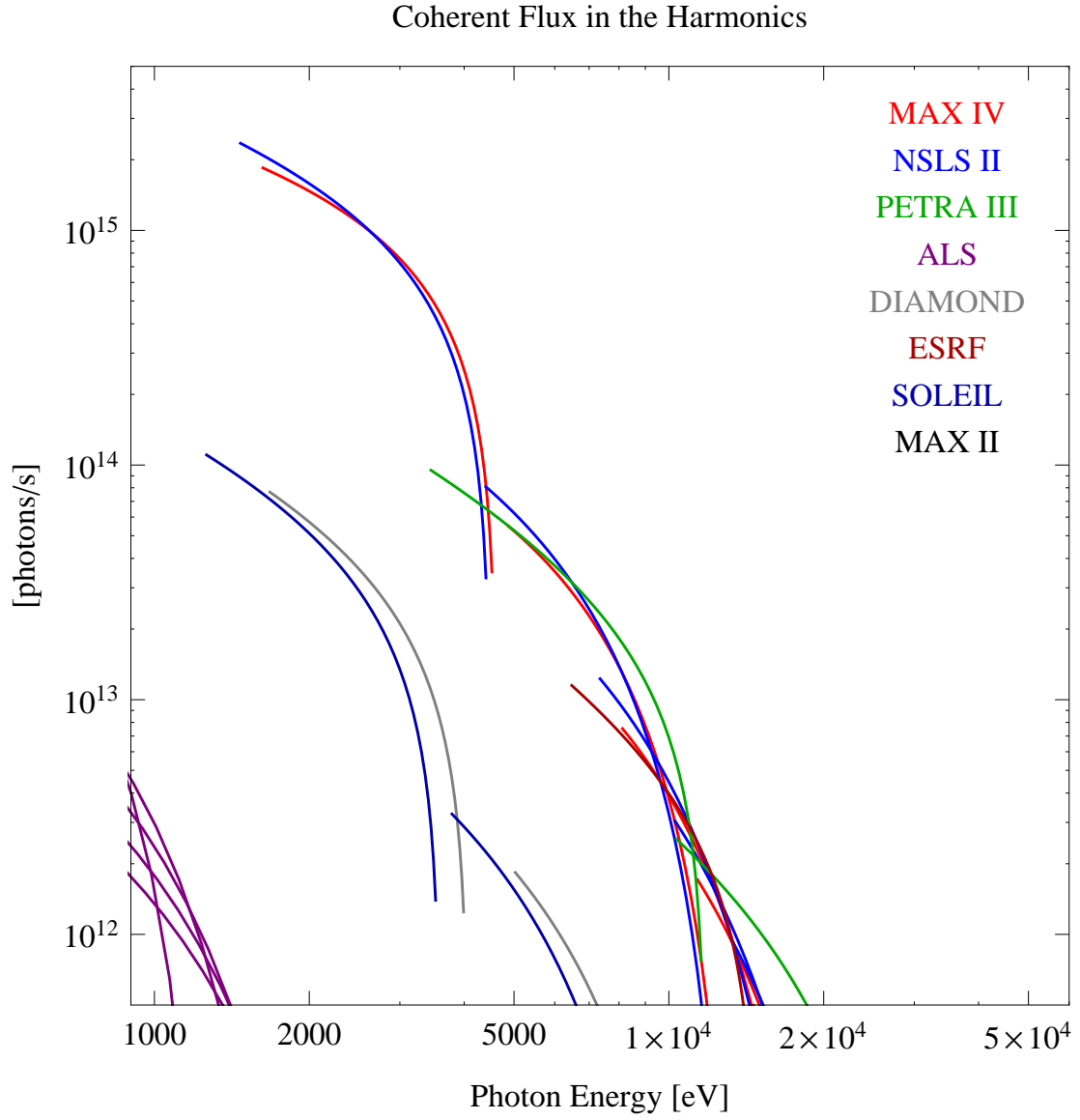


Figure 12: The coherent flux in the harmonics of the the rings and undulators in Table 2

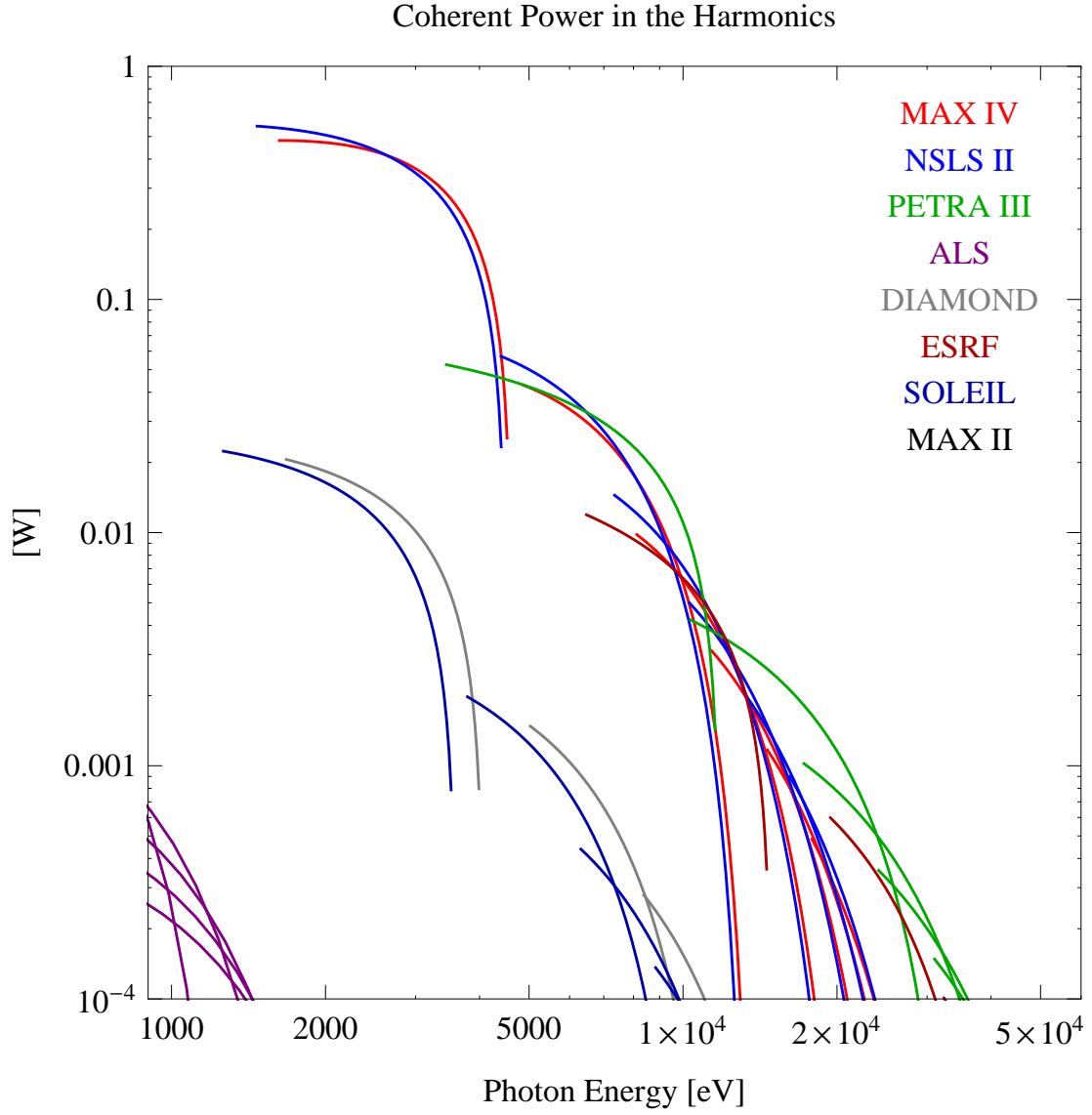


Figure 13: The power of coherent synchrotron radiation in the harmonics of the the rings and undulators in Table 2

References

- [1] K. Balewski, W. Brefeld, W. Decking, H. Franz, R. Rohlsberger, and E. Weckert. PE-TRAI: A Low Emittance Synchrotron Radiation Source, Technical Design Report, February 29, 2004.
- [2] P. Elleaume, J. Chavanne, and B. Faatz. *Nucl. Instr. And Meth. A.*, 455:503–523, 2000.
- [3] MAX IV Detailed Design Report. In preparation. <http://www.maxlab.lu.se/maxlab/max4/index.html>.
- [4] Summary of NSLS-II Source Properties, User Workshop July 17-18, 2007. <http://www.bnl.gov/nsls2/project/>.
- [5] <http://www.als.lbl.gov/als/techspecs/insertdev.html>. ALS Photon Source Parameters.
- [6] <http://www.diamond.ac.uk/Home/Technology/Parameter.html>.
- [7] Reference and information should be updated.
- [8] <http://www.synchrotron-soleil.fr/>.
- [9] M. Sjöström, H. Tarawneh, E. Wallén, and M. Eriksson. Characterisation of the MAX II storage ring lattice. *Nucl. Instr. And Meth. A.*, 577:425436, 2007.

List of Tables

1	Parameters used for the comparison of the brilliance limit at different light sources [3, 4, 1, 5, 6, 7, 8, 9]	4
2	Parameters used for the comparison of specific undulators at different light sources [3, 4, 1, 5, 6, 7, 8, 9]	8

List of Figures

1	Limit at different gaps of the undulator technique used for the comparison of the brilliance limit	3
2	The brilliance limit of the synchrotron radiation storage rings in Table 1	5
3	The angular spectral flux at the brilliance limit of the synchrotron radiation storage rings in Table 1	6
4	The ratio of coherent flux, where the jumps in the curve corresponds to jumps between different harmonic, of the synchrotron radiation storage rings in Table 1	7

5	The brilliance at peak energy of the synchotron radiation emitted at the rings and undulators in Table 2	9
6	The angular spectral flux of the synchotron radiation emitted at the rings and undulators in Table 2	10
7	The flux of photons in the harmonics of the emitted synchrotron radiation at the rings and undulators in Table 2 using a 0.1%BW monochromator .	11
8	The flux of photons in the harmonics of the emitted synchrotron radiation from the rings and undulators in Table 2	13
9	The power in the harmonics of the emitted synchrotron radiation from the rings and undulators in Table 2	14
10	The ratio of coherent flux in the harmonics of the emitted synchrotron radiation from the rings and undulators in Table 2	15
11	The coherent flux in the harmonics of the rings and undulators in Table 2 using a 0.1%BW Monochromator	16
12	The coherent flux in the harmonics of the the rings and undulators in Table 2	17
13	The power of coherent synchrotron radiation in the harmonics of the the rings and undulators in Table 2	18